

Supramolecular Structure of *N,N*-Bis(2-hydroxybenzyl)alkylamine: Flexible Molecular Assembly Framework for Host without Guest and Host with Guest

Suttinun Phongtamrug,[†] Kohji Tashiro,[‡] Mikiji Miyata,[§] and Suwabun Chirachanchai^{*,†}

The Petroleum and Petrochemical College, Chulalongkorn University, Phyathai Road, Pathumwan, Bangkok 10330, Thailand, Department of Future Industry-Oriented Basic Science and Materials, Graduate School of Engineering, Toyota Technological Institute, Tempaku, Nagoya 468-8511, Japan, and Department of Material and Life Science, Graduate School of Engineering, Osaka University, Yamadaoka, Suita, Osaka 565-0871, Japan

Received: March 22, 2006; In Final Form: July 3, 2006

N,N-Bis(2-hydroxybenzyl)alkylamine derivatives form a cage-like assembly consisting of two molecules via inter- and intramolecular hydrogen bonds. The derivatives exhibit themselves as host to accept copper-ion guests under the double-oxygen-bridged dimeric system. Quantum chemical calculation suggested that the host–guest interaction is based on a charge-transfer coordination. Comparison of the crystal structures before and after complexation clarifies a rare example of a host–guest compound where the hosts maintain their cage framework through the change of hydrogen bonds to coordination bonds.

Introduction

Benzoxazine is a unique heterocyclic compound obtained from cyclization between phenol, formaldehyde, and amine.¹ As shown in Scheme 1, theoretically the ring-opening reaction of *p*-substituted phenol-based benzoxazine with phenol derivatives gives a linear aza-methylene-linked phenol-based polymer. We found, however, that the actual reaction tends to terminate at the dimer formation stage, which might be due to the fact that reactive hydroxyl groups are stabilized by inter- and intramolecular hydrogen bonds as reported previously.² The thus-created dimer, *N,N*-bis(2-hydroxybenzyl)alkylamine, hereinafter referred to as **HBA**, takes a cage structure to induce a supramolecular assembly by accepting other molecules or ionic species (Figure 1). As host–guest complexes are known as organometallic catalysts,³ biomimetic metalloproteins,⁴ and enzymatic complex systems,⁵ establishment of **HBA** for supramolecular chemistry might bring useful applications.

In previous papers,^{6,7} we clarified the inclusion phenomena of **HBA** with various guests in either solution or the solid state. It is important to note that parallel to our work there are some reports on **HBA** derivatives with metal ions. For example, Tshuva et al. reported on the zirconium complex of amine-bis-(phenolate) as a candidate catalyst for 1-hexene polymerization.⁸ Malathy Sony et al. showed a biomimetic model complex of *N*-[(2-hydroxylato-5-methyl)benzyl-(2'-hydroxylato-3',5'-dimethylbenzyl)]ethylamine dicopper(II).⁹ Although those complexes demonstrated the precise crystal structures of the **HBA** derivative and metal ions, the role of **HBA** self-assembly and its development to form a complex were not clarified. As we succeeded in preparing a series of **HBA** derivatives via a simple, effective, and selective ring-opening reaction of benzoxazines², it is possible to carry out systematic work on the supramolecular

complex structure under variations of host molecules to establish the supramolecular chemistry of the **HBA**.

In the present article, we focus on two types of benzoxazine dimer derivatives (*N,N*-bis(2-hydroxy-5-methylbenzyl)cyclohexylamine, **HBA1**, and *N,N*-bis(2-hydroxy-3,5-dimethylbenzyl)methylamine, **HBA2**) and on their copper-ion complexation (Scheme 1). On the basis of the information obtained from crystal structure analysis, thermal analysis, vibrational spectroscopy, and quantum chemical calculation, the derivatives have been found for the first time to show their uniqueness in accepting guests without destroying the host framework. This is a rare example among many already revealed hosts. In the present paper, we describe various unique behaviors concerning the specific supramolecular structure of **HBA** on the basis of the following significant experimental findings: (i) the double-oxygen-bridged charge-transfer host–metal complex, (ii) the well-superimposition structure of the hydrogen-bond network of **HBA** and coordination systems of **HBA** with metal guest, and (iii) the existence of multiguest species, i.e., ion and neutral molecules, in a single host–guest framework.

Experimental Section

Preparation of HBA Derivatives. *p*-Cresol, 2,4-dimethylphenol, formaldehyde, methylamine, and cyclohexylamine were obtained from Merck, Germany. Copper(II) acetate monohydrate and sodium hydroxide were purchased from Fluka, Switzerland. 1,4-Dioxane, diethyl ether, 2-propanol, and methanol were from Labscan, Ireland. All chemicals and solvents used for synthesis were of reagent grade and used without purification. *N,N*-Bis(2-hydroxy-5-methylbenzyl)cyclohexylamine (**HBA1**) and *N,N*-bis(2-hydroxy-3,5-dimethylbenzyl)methylamine (**HBA2**) were prepared from a ring-opening reaction of the relevant benzoxazine and phenol derivatives as reported previously.⁷ Mixtures of 3,4-dihydro-6-methyl-3-cyclohexyl-2*H*-1,3-benzoxazine and *p*-cresol (1:1) were prepared and stirred at 60 °C. The mixtures were allowed to react until the solution became viscous, and they were left for precipitation. The precipitates obtained were collected and washed with diethyl

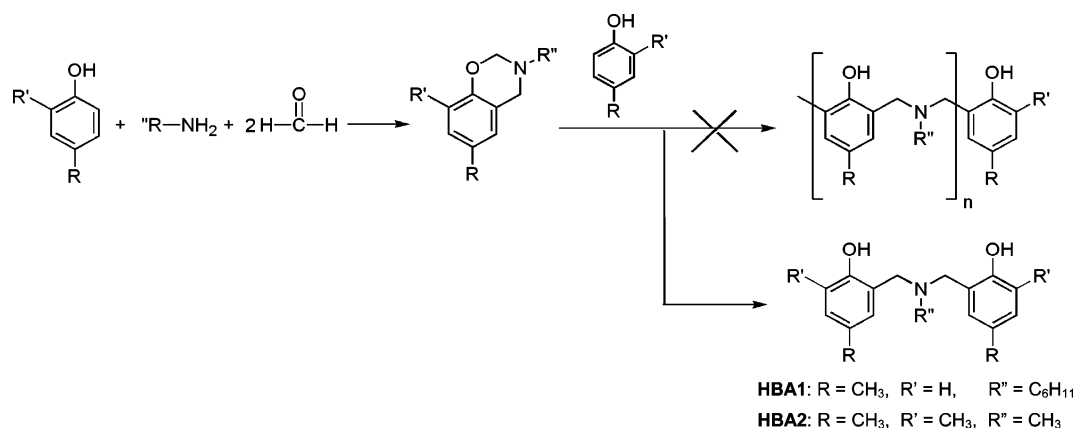
* To whom correspondence should be addressed. E-mail: csuwabun@chula.ac.th.

[†] Chulalongkorn University.

[‡] Toyota Technological Institute.

[§] Osaka University.

SCHEME 1



ether before vacuum drying. **HBA1** was recrystallized in chloroform to prepare single crystals. Similarly, 3,4-dihydro-3,6,8-trimethyl-2*H*-1,3-benzoxazine was reacted with 2,4-dimethylphenol to obtain **HBA2**.

N,N-Bis(2-hydroxy-5-methylbenzyl)cyclohexylamine (**HBA1**): 80% yield; $R_f = 0.30$ (5% MeOH in CHCl_3); clear and colorless solid; mp = 181 °C; FTIR (KBr, cm^{-1}) 3226 (br, OH), 1500 (vs, C=C), 1449 (m, N-CH), 1249 (s, C-N), 1210 (m, C-N-C), 819 (s, C-N-C); ^1H NMR (200 MHz, CDCl_3 , ppm) δ_{H} 1.1 (2H, m, CH_2), 1.45 (4H, m, CH_2), 1.82 (4H, m, CH_2), 2.22 (6H, s, CH_3 -Ar), 2.70 (1H, m, CH), 3.72 (4H, s, Ar- CH_2 -N), 6.68 (2H, d, Ar-H), 6.85 (2H, s, Ar-H), 6.90 (2H, d, Ar-H). Anal. Calcd for $\text{C}_{22}\text{H}_{29}\text{NO}_2$: C, 77.88; H, 8.55; N, 4.13. Found: C, 77.90; H, 8.56; N, 4.16.

N,N-Bis(2-hydroxy-3,5-dimethylbenzyl)methylamine (**HBA2**): 80% yield; $R_f = 0.39$ (5% MeOH in CHCl_3); clear and colorless solid; mp = 123 °C; FTIR (KBr, cm^{-1}) 3399 (br, OH), 1484 (vs, C=C), 1427 (m, N-CH₃), 1243 (m, C-N), 1214 and 1201 (m, C-N-C), 847 (m, C-N-C); ^1H NMR (200 MHz, CDCl_3 , ppm) δ_{H} 2.22 (12H, s, Ar- CH_3), 2.25 (3H, s, N- CH_3), 3.68 (4H, s, Ar- CH_2 -N), 6.72 (2H, s, Ar-H), 6.81 (2H, s, Ar-H). Anal. Calcd for $\text{C}_{19}\text{H}_{25}\text{NO}_2$: C, 76.26; H, 8.36; N, 4.68. Found: C, 76.27; H, 8.34; N, 4.69.

Instrumentation. Fourier transform infrared spectra (FTIR) were recorded by the Nujol mull method in the range 4000–400 cm^{-1} at a resolution of 2 cm^{-1} using a HORIBA FT-720 infrared spectrometer. Thermogravimetric-differential thermal analysis (TG-DTA) was performed with a Rigaku Thermoplus TG8120 from 50 to 300 °C at a heating rate of 5 °C/min under a nitrogen atmosphere.

Structural Analysis. Single crystals of **HBA** with copper ions were prepared by dropping the methanolic copper acetate

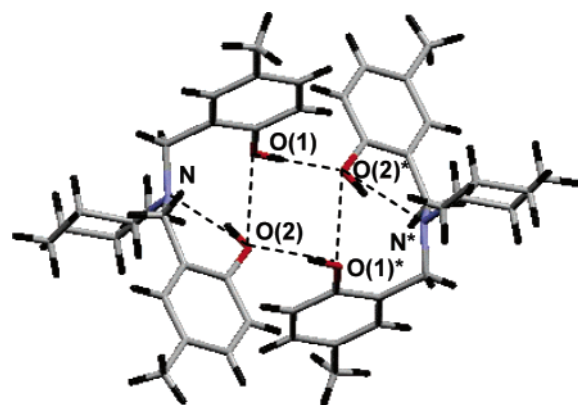


Figure 1. Cage structure of **HBA1** consisting of two **HBA1** molecules (the broken line represents the hydrogen bonds).

solution into methanol solutions of **HBA1** and **HBA2** and leaving them for several days. The single crystals of **HBA** derivatives are colorless, whereas those of the copper inclusions are dark green. X-ray diffraction measurement of **HBA1** and **HBA2** was carried out using an X-ray imaging plate system DIP3000 (MAC Science Co., Ltd., Japan). The graphite monochromatized Mo $\text{K}\alpha$ line ($\lambda = 0.71073$ Å), which was generated from the SRA-M18XHF rotating anode X-ray generator (50 kV and 200 mA), was used as an incident X-ray source. Data correction was performed with XDIP software (MAC Science). The sample was oscillated in a range of 3° over a total rotation angle of 0–180° around the ω axis. The exposure time was 30 min for one image. It took about 12 h to collect the 24 images in total. Data were analyzed using DENZO and SCALEPACK software.^{10,11} The crystal structure was solved using maXus (NoniusBV, Delft) software. The direct method was used to find out the initial models, where the SIR92 software developed by Altomare et al. was used.¹² Least-squares refinement was made on the basis of the full-matrix method using the quantity $\sum \omega(|F_o|^2 - |F_c|^2)^2$ as a minimized function with weight $\omega = \exp[FA \sin^2 \theta / \lambda^2] / [\sigma^2(F_o) + FB F_o^2]$, where $\sigma^2(F_o)$ is the squared standard deviation of the observed structure factor F_o and coefficients FA and FB were set to 0.0 and 0.03, respectively. The reflections satisfying the cutoff condition of $|F_o| > 3\sigma(|F_o|)$ were used in the least-squares refinement. Because no detectable

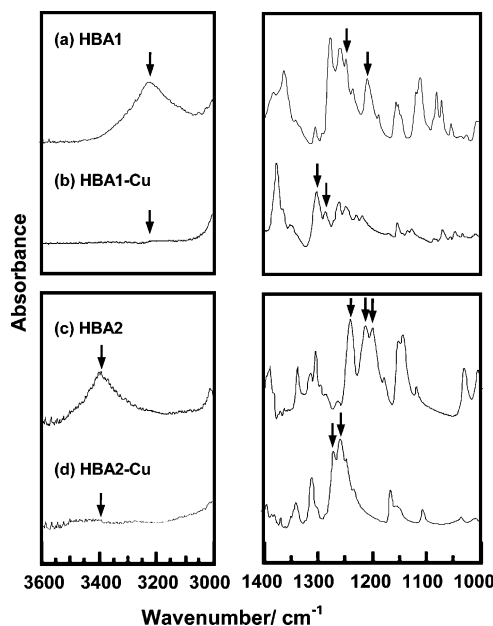


Figure 2. FTIR spectra of (a) **HBA1**, (b) **HBA1**-Cu, (c) **HBA2**, and (d) **HBA2**-Cu after Nujol peaks were subtracted.

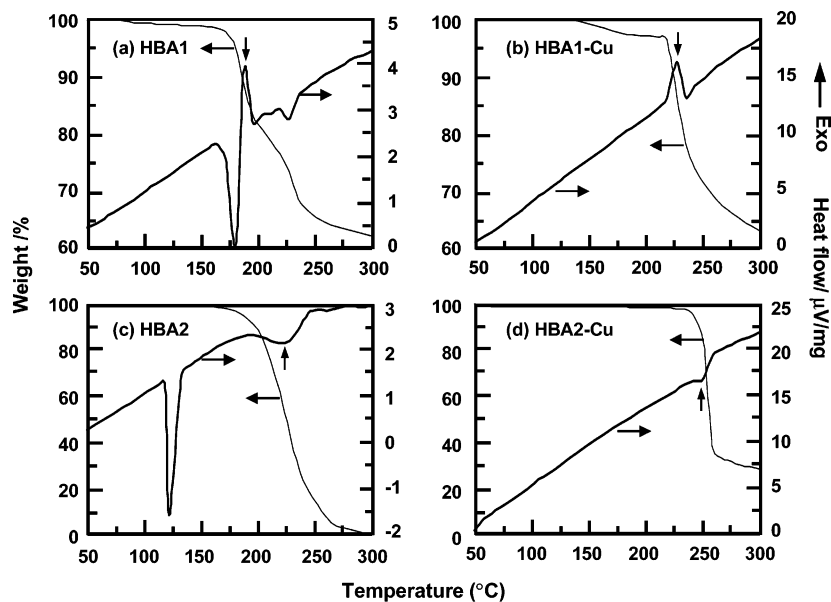


Figure 3. TG and DTA thermograms of (a) **HBA1**, (b) **HBA1**–Cu, (c) **HBA2**, and (d) **HBA2**–Cu.

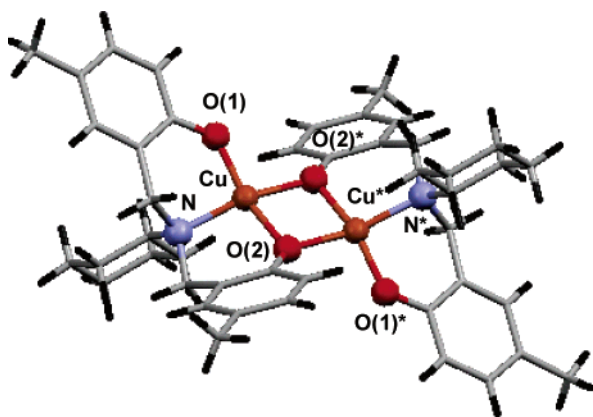


Figure 4. Coordination compound of **HBA1**–Cu.

effect was found, the absorption correction for the observed intensity was not included in the structural refinement. As a measure of the reasonableness of the structural analysis, the reliability factors, R and R_w , were defined by the following equations: $R = \sum ||F_o| - |F_c|| / \sum |F_o|$ and $R_w = [\sum w(|F_o| - |F_c|)^2 / \sum w|F_o|^2]^{1/2}$. X-ray diffraction measurement of **HBA1**–Cu and **HBA2**–Cu was performed using a Rigaku R-Axis RAPID/FS diffractometer with graphite-monochromated Mo K α radiation at 296 K. The structure was solved by direct methods (SIR92)¹² and refined by the full-matrix least-squares procedure on $|F|^2$. All non-hydrogen atoms were refined for anisotropic thermal parameters as well as the coordinates. Hydrogen atoms were detected from the different Fourier map, and positions were refined assuming isotropic thermal parameters. All calculations were performed using the TEXSAN crystallographic software package.¹³

Molecular Modeling. The electron density distribution was calculated for the original cage structure and the complex with Cu ions utilizing DMol³ software (Material Studio, version 3.0, Accelrys) on the basis of density function theory. The atomic orbital basis set was DND (double numerical plus d-functions), and the type of exchange-correlation potential was a local LDA. The molecular structures were transferred directly from the X-ray analysis results, and electron densities were calculated for the isolated molecules without energy optimization.

Results and Discussion

Infrared Spectral Change by Cu Complexation. Green crystals of **HBA1** and **HBA2** including copper ions, abbreviated as **HBA1**–Cu and **HBA2**–Cu, were characterized by FTIR to observe the vibrational spectral changes caused by copper inclusion. Since metal-ion exchange might occur relatively easily when KBr powder is mixed with **HBA1**–Cu and **HBA2**–Cu complexes, samples for IR measurements were prepared by the Nujol mull method. Figure 2 shows the FTIR spectra of the single crystals of **HBA1**, **HBA2**, and their copper inclusions where the contribution of Nujol bands was already subtracted. Although **HBA1** and **HBA2** give the peak positions and width of the bands differently, due to the strength and environment of the hydrogen bonds, the OH peaks are clearly observed before complex formation for both compounds (Figure 2a and 2c). After entrapping copper ions, the significant decrease of the OH band intensity was observed, as shown in Figure 2b and 2d, corresponding to loss of inter- and intramolecular hydrogen bonds. This implies that **HBA1** and **HBA2** form a complex with copper ions. The newly observed peaks for **HBA1**–Cu (Figure 2b) are at 1305 and 1289 cm^{−1}, whereas for **HBA2**–Cu (Figure 2d) they are at 1267 and 1255 cm^{−1}.¹⁴ These bands may be assigned to the C–N vibrational modes. However, these are different from the usual ones at 1249 and 1210 cm^{−1} for **HBA1** and at 1243, 1214, and 1201 for **HBA2**. This result indicates the change of the vibrational mode of the aza group after copper-ion inclusion. In this way, the OH and C–N groups of **HBA** were affected remarkably by introducing copper ions.

Thermal Stability of Complex. Thermal stabilities of the compounds before and after inclusion of the copper ion were investigated. As shown in Figure 3a, **HBA1** gives a sharp melting at 177 °C followed by an exothermic peak at 185 °C and an endothermic peak at 225–240 °C with a remarkable weight loss. As the measurement was done in a nitrogen atmosphere, the endothermic peak reflects the continuous thermal degradation in nonoxidative conditions. However, in the case of **HBA1**–Cu, the melting peak was difficult to detect and only an exothermic peak due to thermal degradation was observed (Figure 3b). For **HBA2**, the melting peak was located at 125 °C and it disappeared after complexation (Figure 3c and 3d). Thermal degradation of **HBA2** was observed at 225 °C, whereas that of **HBA2**–Cu was identified at 250 °C. The

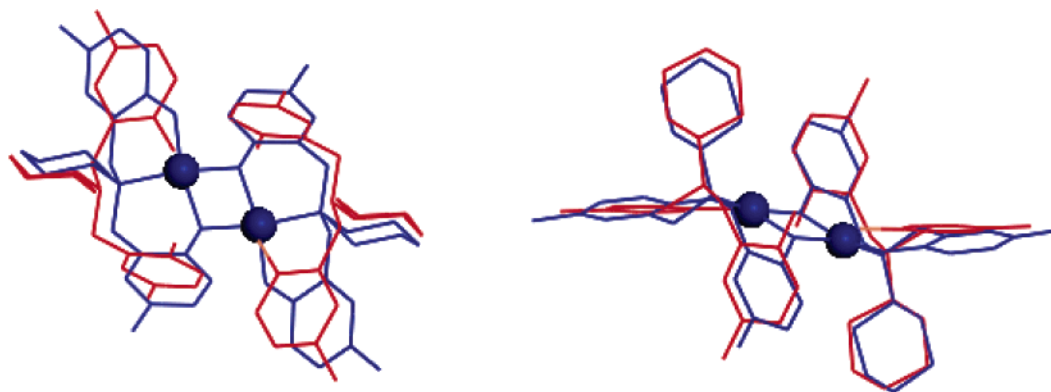
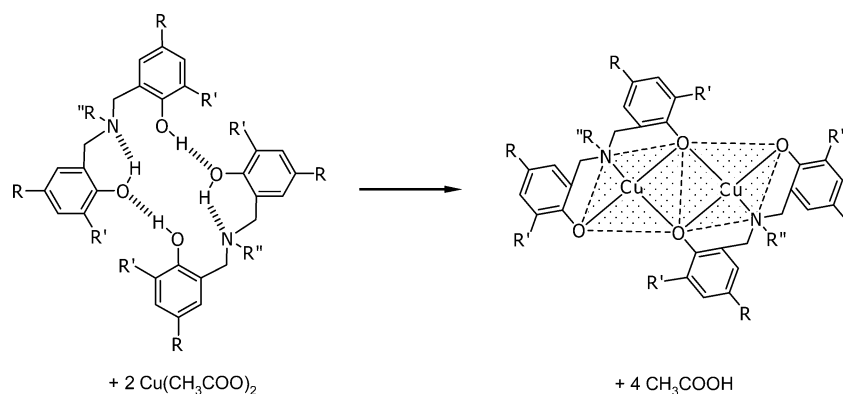


Figure 5. Comparison of cage structure between **HBA1** (red color) and **HBA1**–Cu complex (blue color) viewed from different directions.

SCHEME 2



increase in thermal degradation indicates a remarkable thermal stability of the **HBA1** and **HBA2** complexes.

Crystal Structures. To clarify the crystal structures of the **HBA**–copper complexes, single-crystal X-ray analysis was performed. Figure 4 shows the inclusion structure of **HBA1**–Cu with doubly bridged Cu–oxygen linkages. Each copper is bridged by three phenoxy oxygens and an amine donor. The bond lengths of Cu–O(1), Cu–O(2), Cu–O(2)*, and Cu–N are almost identical (1.85–2.05 Å). These distances are in the range suitable for stable Cu–O and Cu–N coordination bonds.¹⁵ The bond angles of O(1)–Cu–N, O(2)–Cu–N, O(1)–Cu–O(2)*, and O(2)–Cu–O(2)* are nearly 90°, as illustrated in Scheme 2, and therefore, the inclusion structure appears in a distorted square-planar geometry. Similar coordination is also identified for other types of asymmetric hydroxybenzylalkylamine with different substituted groups (R, R', and R'' in Scheme 1) including the derivatives reported previously.⁹ This type of molecular geometry was reported also by Malathy Sony et al.⁹ It is important to note that the square-planar geometry is a unique characteristic of the **HBA** derivatives, which form coordination bonds with metals.

Although, in general, it is difficult to determine the proton positions by single-crystal X-ray analysis, we succeeded in extracting the protons of OH groups for **HBA1** and **HBA2** with reasonable bond distances. In the case of **HBA1**–Cu, however, the hydrogen atoms could not be detected but the oxygen atoms were found to be directly linked to Cu atoms, as shown in Figure 4. Here, we could not identify the acetate counteranions, although there were reports that inclusion complexes occasionally show their counterions.¹⁶ This causes us to speculate that the hydrogen atoms of the hydroxyl groups might perform as proton donors for acetate anions, resulting in formation of acetic acid molecules after complexation (Scheme 2). This speculation is consistent with the infrared spectrum (Figure 2) in which

O–H stretching at 3200–3400 cm^{−1} is hardly observed for the **HBA1**–Cu complex.

As shown in Figure 1, the **HBA** derivatives form the inter- and intramolecular hydrogen bonds between N atoms and OH groups (O(1)–H···O(2)* and N···H–O(2)), resulting in an assembly of two **HBA** molecules.² As for the **HBA** with and without guest ions, the point to be raised here is that the cage is formed between the two **HBA** molecules either before or after complex formation (Scheme 2). As described later, the electron density distribution was calculated for the original cage structure and the complex with Cu ions on the basis of density function theory utilizing DMol³ software. As demonstrated in Figure 5, the size and shape of the cage structure composed of two **HBA** molecules are maintained even after complexation with Cu ions, although the O–H···O and O–H···N inter- and intramolecular hydrogen bonds, respectively, are replaced with coordination linkages of Cu–O and Cu–N types. This geometrical relation between the **HBA** and **HBA**–Cu complex may allow us to speculate on the mechanism of benzoxazine–copper complex formation (as discussed later).

Stabilization of Supramolecular Structure by Solvent Molecules. Such a reservation of cage structure can also be seen for **HBA2**–Cu complexation (Figure 6). However, it is important to note that complexation of **HBA2** is a little different from that of **HBA1**.¹⁷ As shown in Figure 7, three water molecules are coexistent with the dimeric **HBA2**–Cu molecules in the crystal lattice. The distances between the phenoxy oxygens (O(3)–H···O(1)) and water oxygens (O(4)–H···O(3)) are 2.70 and 2.82 Å, respectively. The positions of the hydrogen atom belonging to the water molecules were extracted successfully from the difference Fourier synthesis map. The O(1)···H distance is 1.78 Å, which is acceptable for the interatomic distance of the hydrogen bond, as found for cases of phenol and water (1.80 Å).¹⁸ The structure reveals that **HBA2**–Cu

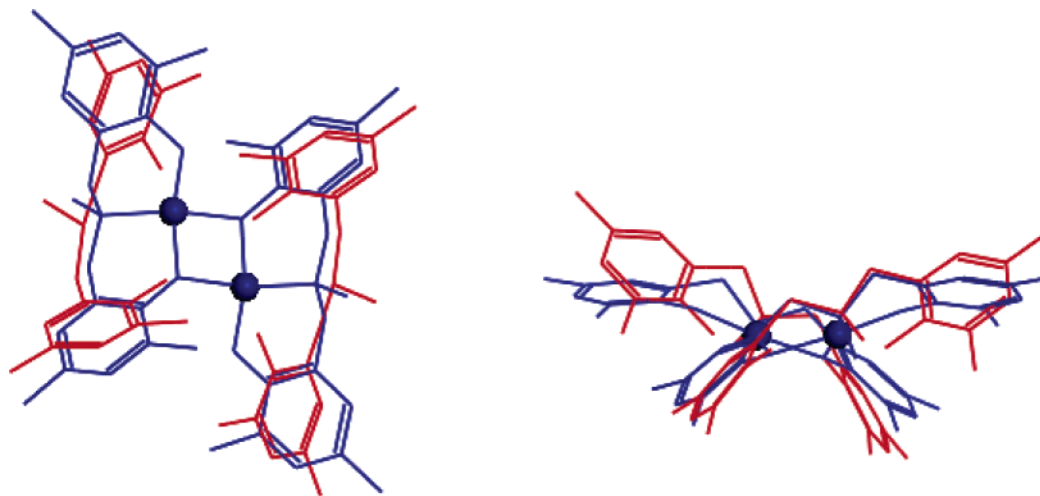


Figure 6. Comparison of cage structure between **HBA2** and **HBA2**–Cu viewed from different directions.

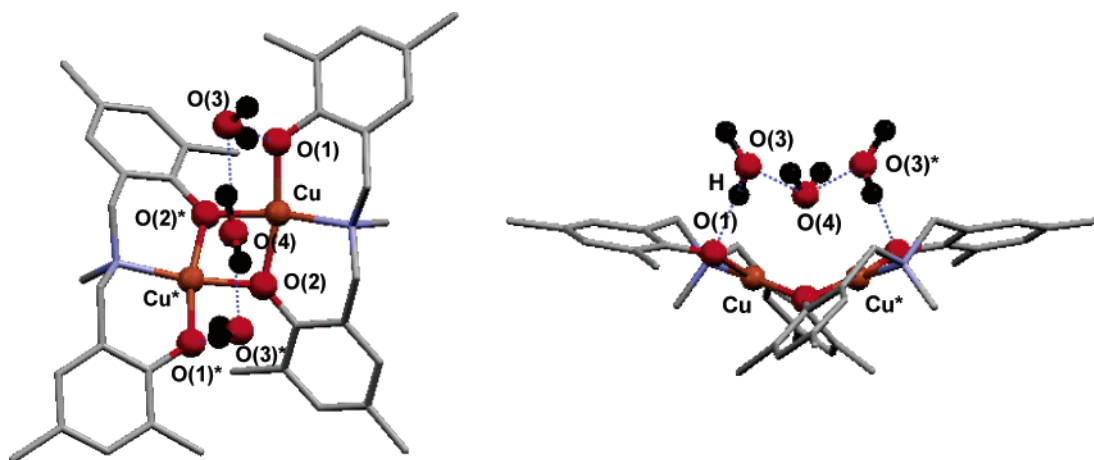


Figure 7. Structure of **HBA2**–Cu complex coordinated by water molecules. (Hydrogen atoms are omitted for clarity.)

complex takes a unique bowl-shaped network structure and accepts those small solvent molecules to stabilize the whole structure.

Comparison of crystal volumes also supports this concept about the role of the water molecules in formation of **HBA2**–Cu complex. For **HBA2**–Cu, one complex framework composed of the two **HBA2** molecules has a volume of 963.6 Å³ whereas a single **HBA2** framework has a volume of 859.1 Å³. This volume increment after Cu-complex formation is different from that of **HBA1**, showing a decrease in volume after complexation from 974.1 to 959.9 Å³.

Essential Features of Benzoxazine–Copper Complexes.

The characteristic features of these copper complexes of **HBA** are seen in the formation of the double square planes connected by common oxygen atoms. To reveal the characteristic features, the atomic charge distribution was calculated on the basis of density function theory with DMol³ (Material Studio Version 3.0, Accelrys). The atomic orbital basis set was DND (double numerical plus d-functions), and the type of exchange–correlation potential was a local LDA. In the calculation the X-ray-analyzed structure was used without any further optimization. Of course, it is more ideal to take the intermolecular interactions into account in the geometrical calculation, but the DFT calculation of the whole crystal lattice is quite a hard task for such a complicated structure, as in the present case. The calculation was made for a rough estimation of the atomic charge distribution in this characteristic complex structure. More detailed and accurate calculation will be made in the future to clarify the

essence of the charge distribution change in the formation process of the complex crystal, and it is also expected that the infrared frequencies and intensities obtained from the calculation will support the results in Figure 2.

Figure 8 shows the calculated electrostatic potential (ESP) charges. In the case of **HBA1**, the typical charge distribution is observed for the O–H···O hydrogen bond. After complexation (Figure 8b), the charges of oxygen atoms connected directly to the Cu atom change from –0.47 and –0.58 to –0.53 and –0.78 eV. At the same time the charges of nitrogen atoms decrease from –0.34 to –0.55 eV. The phenol carbon atoms connected to oxygen also change their charges. As for the Cu atom, the charge decreases from +2 (Cu²⁺ of Cu(CH₃COO)₂) to +1.02 is shown in Figure 8b. The changes in the atomic charge distribution suggest that the electrons flow from carbon (or aromatic rings) to oxygen and nitrogen and to copper atoms. Referring to the case of π -conjugated oligo(phenylene ethynylene),¹⁹ we speculate that our complex might be formed by the charge-transfer mechanism. Considering the assembly networks of **HBA1** and **HBA2**, it is natural to emphasize that the charge-transfer coordination networks of **HBA1**–Cu and **HBA2**–Cu are formed with only a minor destruction of the original packing structure. In other words, the charge-transfer complex is initiated smoothly by substituting the hydrogen atoms with Cu atoms. This type of dimeric charge-transfer complexation is, to our knowledge, quite rare to find in general complexation.

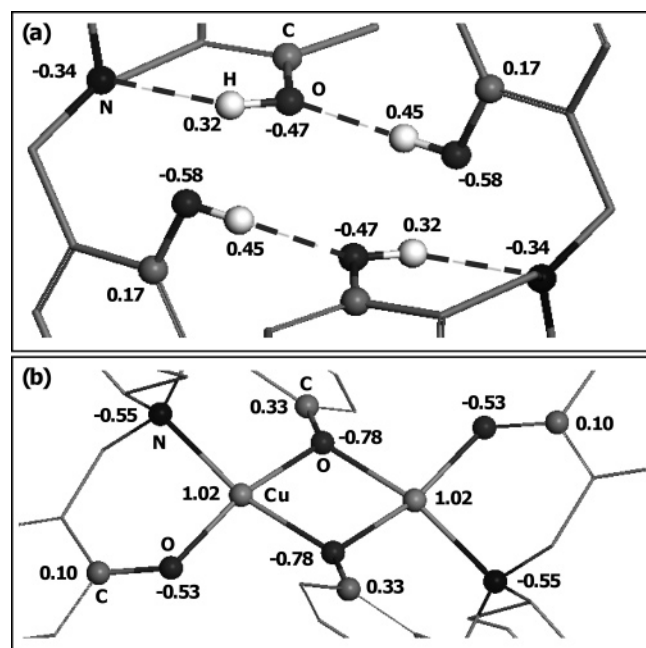


Figure 8. Calculated atomic charges of (a) **HBA1** and (b) **HBA1-Cu**.

Conclusions

In general, a host molecule accepts a guest species under the interaction induced by favorable conditions, e.g., solvent dissolution, melting, and irradiation. To date, it is known that the host likely dissolves its original framework and establishes its new channel to incorporate the guest. The present work clarified a unique type of complex formation in that the host retains its framework even after accepting guests: **HBA1** and **HBA2** form complexes with copper ions without losing the cage-like structure through modification from a hydrogen-bonded self-assembly to a coordination-bonded host-guest system, as illustrated in Scheme 2. The energy calculation suggested formation of an **HBA**-copper complex through the atomic charge transfer among the phenoxy oxygen atom, aromatic ring, and aza methylene group, leading to a double-oxygen-bridged network.

Acknowledgment. One of the authors, S.C., acknowledges financial support from The Thailand Research Fund (grant no. RSA4680025) and extends his appreciation for the support from the Hitachi Scholarship Foundation. The authors gratefully thank Mr. Katsunari Inoue (Graduate School of Engineering, Osaka University, Japan) for help in single-crystal analysis.

Supporting Information Available: Crystallographic information files (CIF); **HBA1**, **HBA2**, **HBA1-Cu**; CCDC 258998, and **HBA2-Cu**; CCDC 258999. This material is available free of charge via the Internet at <http://pubs.acs.org>.

References and Notes

- (1) (a) Sainsbury, M. *Comprehensive Heterocyclic Chemistry: The Structure, Reactions, Synthesis and Uses of Heterocyclic Compounds, Part 2B: Six-membered Rings with Oxygen, Sulfur, or Two or More Nitrogen Atoms*; Boulton, A. J., McMillan, A., Eds.; Pergamon Press: United Kingdom, 1984. (b) Holly, F. W.; Cope, A. C. *J. Am. Chem. Soc.* **1944**, *66*, 1875–1879. (c) Burke, W. J.; Hammer, C. R.; Weatherbee, C. J. *Org. Chem.* **1961**, *26*, 4403–4407.
- (2) Laobuthee, A.; Chirachanchai, S.; Ishida, H.; Tashiro, K. *J. Am. Chem. Soc.* **2001**, *123*, 9947–9955.
- (3) (a) Stibrany, R. T.; Schulz, D. N.; Kacker, S.; Patil, A. O.; Baugh, L. S.; Rucker, S. P.; Zushma, S.; Berluche, E.; Sissano, J. A. *Macromolecules* **2003**, *36*, 8584–8586. (b) Evans, D. A.; Seidel, D.; Rueping, M.; Lam, H. W.; Shaw, J. T.; Downey, C. W. *J. Am. Chem. Soc.* **2003**, *125*, 12692–12693. (c) Takacs, J. M.; Reddy, S.; Moteki, S. A.; Wu, D.; Palencia, H. J. *Am. Chem. Soc.* **2004**, *126*, 4494–4495.
- (4) Itoh, S.; Taki, M.; Kumei, H.; Takayama, S.; Nagatomo, S.; Kitagawa, T.; Sakurada, N.; Arakawa, R.; Fukuzumi, S. *Inorg. Chem.* **2000**, *39*, 3708–3711.
- (5) Lubben, M.; Hage, R.; Meetsma, A.; Byma, K.; Feringa, B. L. *Inorg. Chem.* **1995**, *34*, 2217–2224.
- (6) Laobuthee, A.; Ishida, H.; Chirachanchai, S. *J. Incl. Phenom. Macrocyclic Chem.* **2003**, *47*, 179–185.
- (7) Phongtamrug, S.; Pulpoka, B.; Chirachanchai, S. *Supramol. Chem.* **2004**, *16*, 269–278.
- (8) Tshuva, E. Y.; Goldberg, I.; Kol, M.; Goldschmidt, Z. *Organo-metallics* **2001**, *20*, 3017–3028.
- (9) Malathy Sony, S. M.; Kuppavey, M.; Ponnuswamy, M. N.; Manonmani, J.; Kandasamy, M.; Fun, H.-K. *Cryst. Res. Technol.* **2002**, *37*, 1360–1367.
- (10) Otwinowski, Z.; Minor, W. *Methods Enzymol.* **1997**, *276*.
- (11) Otwinowski, Z.; Minor, W. *Macromolecular Crystallography: Part A*; Carter, C. W., Jr., Sweet, R. M., Eds.; Academic Press: London, 1997.
- (12) Altomare, A.; Cascarano, G.; Giacovazzo, C.; Guagliardi, A.; Burla, M. C.; Polidori, G.; Camalli, M. *J. Appl. Crystallogr.* **1994**, *27*, 435.
- (13) *TEXSAN, X-ray Structure Analysis Package*; Molecular Structure Corp.: The Woodlands, TX, 1985.
- (14) Silverstein, R. M.; Bassler, G. C.; Morrill, T. C. *Spectrometric Identification of Organic Compounds*; John Wiley & Son, Inc.: New York, 1991.
- (15) Murphy, B. P. *Coord. Chem. Rev.* **1993**, *124*, 63–105.
- (16) (a) Ozbey, S.; Kendi, E.; Hosgoren, H.; Togrul, M. *J. Inclusion Phenom. Mol. Recognit. Chem.* **1998**, *30*, 79–87. (b) Amani Komaei, S.; van Albada, G. A.; Haasnoot, J. G.; Kooijman, H.; Spek, A. L.; Reedijk, J. *Inorg. Chim. Acta* **1999**, *286*, 24–29. (c) Helm, M. L.; Loveday, K. D.; Combs, C. M.; Bentzen, E. L.; VanDerveer, D. G.; Rogers, R. D.; Grant, G. J. *J. Chem. Crystallogr.* **2003**, *33*, 447–455. (d) Knaust, J. M.; Knight, D. A.; Keller, S. W. *J. Chem. Crystallogr.* **2003**, *33*, 813–823.
- (17) Phongtamrug, S.; Miyata, M.; Chirachanchai, S. *Chem. Lett.* **2005**, *34*, 634–635.
- (18) Guedes, R. C.; Coutinho, K.; Cabral, B. J. C.; Canuto, S. *J. Phys. Chem. B* **2003**, *107*, 4304–4310.
- (19) Majumder, C.; Briere, T.; Mizuseki, H.; Kawazoe, Y. *J. Chem. Phys.* **2002**, *117*, 7669–7675.